17th World Conference on Earthquake Engineering, 17WCEE
Sendai, Japan - September 13th to 18th 2020

CALIBRATING A CONSTITUTIVE NONLINEAR MATERIAL MODEL FOR STONE MASONRY IN MUD MORTAR WALLS IN NEPAL

J. Meadows(1), L. Shrestha(2), D. R. Paudel(3)

(1) *Senior Engineer, Robert Bird Group/Build Change Nepal, joelmeadows@gmail.com*
(2) *Lead Structural Engineer, Build Change Nepal, liva@buildchange.org*
(3) *Technical Resource Development – Team Leader, Build Change Nepal, dev@buildchange.org*

Abstract

The 2015 Gorkha earthquake in Nepal caused devastating damage across the country, with entire villages affected and hundreds of thousands of people left homeless. This calamitous natural disaster highlighted the seismic vulnerability of traditional uncoursed random rubble walls built from stone masonry in mud mortar, which are common in rural areas of Nepal, and focused the attention of researchers and structural engineers on improving their knowledge of these materials. This paper addresses this problem and investigates the effectiveness of a retrofit design which is currently being used to strengthen traditional buildings in Nepal.

An experimental campaign was carried out at the Tribhuvan University in Nepal in accordance with the ASTM Standards [1] including uniaxial compression tests, combined axial and shear tests, and diagonal compression tests on both traditional masonry samples and samples which had been retrofitted with concrete plaster on each face and a reinforced concrete element through the centre. The uniaxial compression tests allowed for the compressive strength, modulus of elasticity and the normal stress-normal strain relationships to be determined and the failure patterns and mechanisms were recorded. The combined axial and shear tests and the diagonal compression tests allowed for the shear strength, tensile strength and crack patterns to be evaluated. Due to the low bond strength of the masonry samples, the standard diagonal compression test method was modified such that the wall panels were built oriented vertically and the loading mechanism was rotated 45 degrees, rather than the opposite. Earlier numerical analyses have demonstrated that it is possible to neglect the influence of this modification. [2]

A finite element investigation was then carried out using a nonlinear modelling procedure (smeared crack approach) with the aim of replicating the experimental results in numerical simulations. Due to the random nature of stone masonry in mud mortar wall construction, a macro-modelling approach was adopted and three-dimensional finite element models of the laboratory experiments were created in ANSYS with the aim of replicating the plastic deformation and failure mechanisms. This finite element analysis involved calibrating a nonlinear constitutive material model, combining Drucker-Prager plasticity and Willam-Warnke failure criteria. This constitutive material model has previously been used by other researchers to simulate the behaviour of masonry materials [3, 4]. The Drucker-Prager model controls the plasticity of the material and is calibrated by adjusting parameters related to cohesion, the angle of internal friction and the dilatancy angle, while the Willam-Warnke model controls when failure occurs by defining the material tensile and compressive strength.

The parameters of the material model were initially set to values either calculated from the experimental results or based on a wide literature review, with a subsequent sensitivity analysis used to see how varying each of the parameters changed the behaviour of the material. Based on this sensitivity analysis the material models were then calibrated until the numerical analysis results closely matched the laboratory experiment results. This included both the plastic nonlinear behaviour of the samples and the brittle failure mechanisms, including a close correlation in crack patterns. Furthermore, this analysis showed that the retrofit solution was effective at increasing the in-plane seismic capacity of the wall significantly by improving its tensile strength. The findings from this paper could also be used to carry out nonlinear analysis on models of traditional buildings to better understand their responses to seismic forces.

Keywords: Stone masonry with mud mortar; constitutive material model; Drucker-Prager; Willam-Warnke; ANSYS

1. Introduction

The 2015 Gorkha earthquake highlighted the seismic vulnerability of uncoursed random rubble structures built from stone masonry in mud mortar (SMM), which are very common in rural areas of Nepal. Unfortunately, very little research on the material properties of these structures has been carried out to date which makes evaluating their seismic capacity very difficult. Following the devastating earthquake Build Change began work in Kathmandu and over the last few years developed a retrofit design that can be used on SMM buildings with various dimensions. The purpose of the research presented here is to calibrate a set of validated parameters to describe the mechanical behaviour of traditional masonry walls in Nepal, so that the seismic capacity of existing buildings can be accurately determined, thus allowing for the design of targeted seismic retrofitting works.

To determine accurate values for the mechanical characteristics of SMM, Build Change engineers carried out a number of laboratory experiments including uniaxial compression tests, combined axial and shear tests, and diagonal compression tests. The results from these tests allowed for important material properties such as the Young's modulus, compressive capacity, tensile capacity and shear capacity to be determined. Although several past research projects have been performed on SMM wall components [5], only one comparable research study is available for traditional stone masonry in mud mortar buildings in Nepal, and it used the results from Build Change's laboratory experiments. [6] Validated material properties are also very important for the development of numerical models, which are routinely used to simulate the response of structures to seismic forces. As SMM exhibits a significant nonlinear response, even at relatively low loads, it was decided to carry out nonlinear numerical analyses in ANSYS to simulate the laboratory experiments. By adjusting the material properties in the finite element analysis (FEA), a constitutive nonlinear material model was calibrated which matched the experimental results with a sufficient degree of accuracy.

1.1 Characterisation of SMM Walls

Most buildings in rural areas of Nepal are constructed using load bearing walls constructed from uncoursed random rubble stone masonry in mud mortar with an approximate thickness of 450mm. The number of storeys varies from one to three, with the most typical arrangement being a two-storey building as shown in Fig. 1. The attic floor is supported by an internal timber frame with a row of central timber columns supporting a primary longitudinal beam, with transverse joists spanning out to the side walls.

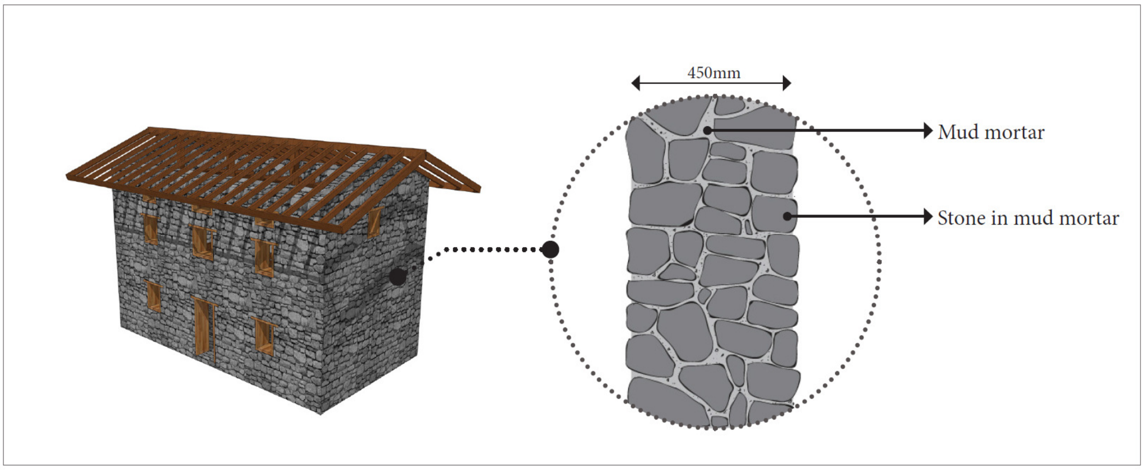

Fig. 1 – A typical traditional Nepalese house (left) and a section through a SMM wall (right).

As the materials are locally sourced, and mason skill and construction preferences change by region, there is a lot of variability in construction across Nepal, as shown in [6]. In order to ensure consistency when comparing the results of each experiment Build Change employed masons from the Kavrepalanchowk district, where a significant proportion of houses are built using stone masonry in mud mortar. The masons were very familiar with this construction technique and they used roughly cut stones and mud mortar with two or three weakly connected wythes (Fig. 2).

The stones are placed in a systematic manner to obtain a flat surface and avoid any voids between them, in such a way that the mortar thickness is as small as possible. The retrofitted samples were built in exactly the same way as the existing samples except that 28 days after the wall had been built, a reinforced “through concrete” element was built into the middle of the panel and a 25-30mm thick cement plaster layer was applied to both faces of the panel, to replicate the order and method in which retrofits are usually carried out in the field. All of the samples with concrete elements were then left to cure for an additional 28 days.

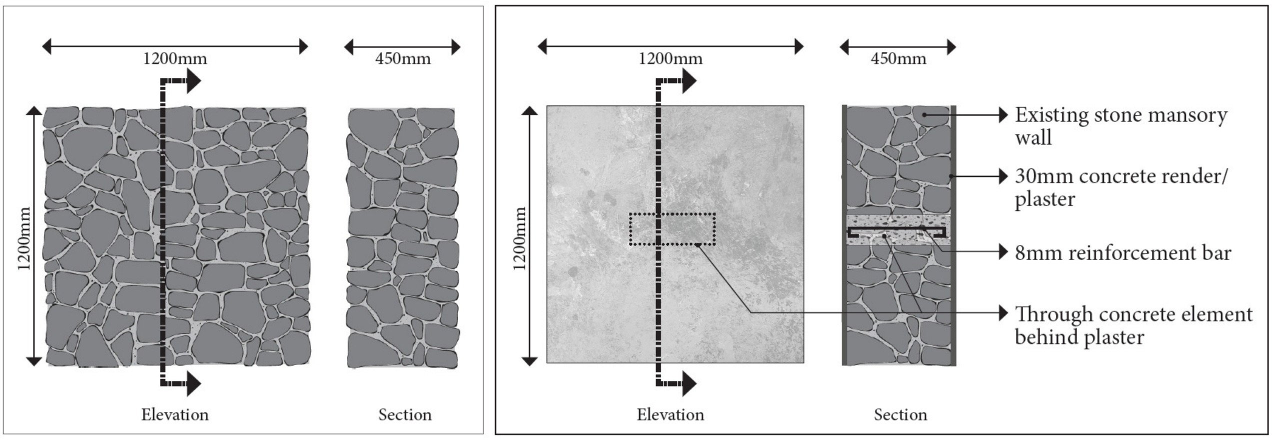

Fig. 2 – Relief of the different panels tested: existing SMM wall (left) and retrofitted SMM Wall (right).

2 Experimental Test Campaign and Analysis

An experimental campaign was carried out at the Pulchowk Engineering College in Kathmandu, including uniaxial compression tests, combined axial and shear tests, and diagonal compression tests, in order to determine the elastic modulus, compressive strength, shear strength and tensile strength of the samples. As noted above, the existing SMM wall samples were tested 28 days after their construction and the retrofitted samples were tested 28 days after the addition of the through concrete elements and cement plaster.

Fig. 3 – Uniaxial compression test setup (left), combined axial and shear test (middle) and diagonal compression test (right).

2.1 Uniaxial Compression Test

This test was designed to examine the behaviour of mud mortar stone wallets in compression. Design parameters such as compressive strength, modulus of elasticity and the normal stress-normal strain relationships were determined and the failure patterns and mechanisms developed in uniaxial loading were recorded. Three un-retrofitted test samples were prepared according to ASTM C1314 [7] with height to thickness ratios between 1.3 and 5. The aim was to construct all of the samples with the same dimensions but due to the irregularity of the stones, there were some small differences in dimensions between the wallets.

The top of the wallets were capped with cement slurry, to provide a flat surface for the application of axial compression load. Metal plates were also used on top of the cement slurry to ensure that the load was applied equally over the wallet. The tests were carried out on a Universal Testing Machine (UTM), with the vertical displacement recorded by a displacement gauge fixed to the loading plate of the UTM. The ultimate load was recorded and the behaviour of the wall (damage patterns) under different loads was also observed and recorded. The modulus of elasticity was estimated by reviewing the linear elastic domain of the stress-strain plot, which generally reached up to about one third of the compressive strength.

Table 1 – The uniaxial compression test sample dimensions

Sample	Thickness (mm)	Width (mm)	Height (mm)	Compressive Strength (MPa)	Young's Modulus (MPa)
1	350	450	540	2.33	66.4
2	375	455	540	2.68	64.3
3	370	475	540	2.01	57.5
Average	365	460	540	2.34	62.7

The type of failure observed in the samples was brittle failure, with cracks forming first in the mortar joints and then later in the stones. Cracking first occurred at roughly 50% of the ultimate compression force and as the samples approached their ultimate compression capacity, the displacement measured increased dramatically leading to the collapse of the samples. Delamination of the wythes was commonly observed as a collapse mechanism.

2.2 Combined Axial and Shear Test

The samples were prepared according to ASTM C-1314 [7] with a panel size of 1.2m x 1.2m and a wall thickness of 0.45m. This test was designed to examine the behaviour of a typical existing stone wall under the combined effect of constant axial load and cyclic lateral loading. While this test is a cyclic test with the load being applied from alternate sides consecutively in order to generate a hysteretic plot, for the purposes of this paper the results from applying the force in only one direction were used for the calibration exercise. The results from this laboratory experiment are shown in Fig. 4.

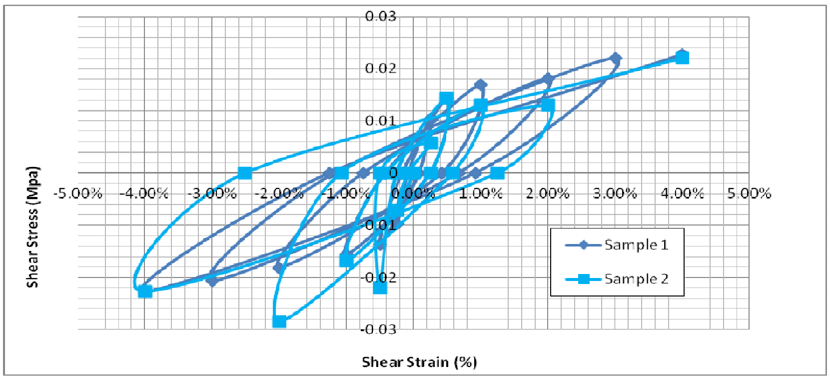

Fig. 4 – Shear Stress/Shear Strain experimental results for the two combined axial and shear test samples.

2.3 Diagonal Compression Tests

Diagonal compression tests were also carried out in accordance with ASTM E519-07 [1] to evaluate the shear strength and tensile strength of SMM walls and walls which had been retrofitted. These tests were performed on 1.2 x 1.2 m square panels characterised by a thickness of 0.45m, reflecting the typical thickness of traditional SMM walls in Nepal.

The ASTM Standard test requires that the sample is built on a 45° angle and that the load is applied vertically, as shown in Fig. 5. However, due to the low masonry bond strength of the traditional SMM wall panels, the standard test method was modified such that the wall panel remained vertical and the loading mechanism was rotated by 45° as shown in Fig. 5. Loading was applied by a hydraulic cylinder positioned between the steel beam and the sample, which when loaded developed tension forces in the four steel rods positioned between the steel beams, consequently compressing the wall panel diagonally. The applied diagonal compression force was increased gradually in 1 kN increments until failure occurred in the wall panel. Deformation of the wall panels was measured primarily by recording the extension of the hydraulic cylinder and measuring tapes were also used to record the diagonal dimensions of both sides of the sample for each load increase. Numerical analyses have demonstrated that it is possible to neglect the influence of the adjusted experimental setup. [2]

The results from the diagonal compression tests were used to determine the shear and tensile capacity of the samples, based on when failure of the samples was observed. Using the formula derived from a linearly elastic analysis of the panel considered as a homogenous solid by [8], an average tensile strength of 0.02 MPa for the existing SMM walls and 0.056 MPa for the retrofitted samples was calculated. As summarised in Table 2, the tensile capacity of the retrofitted samples was found to be approximately three times greater than that of the existing SMM walls.

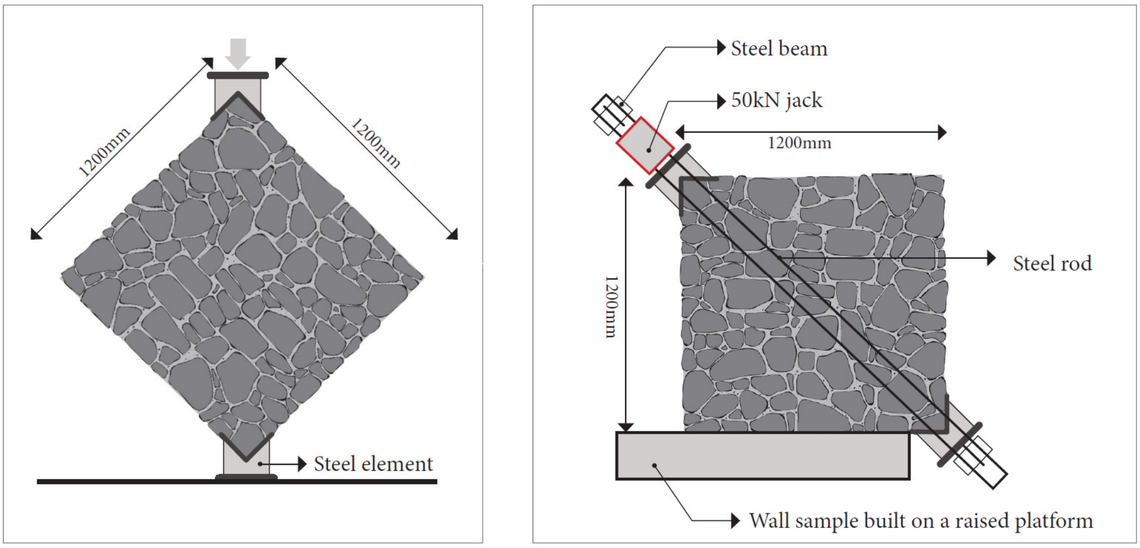

Fig. 5 – ASTM test setup (left) and revised setup (right).

Table 2 – Experimental results of the Diagonal Compression Tests.

Sample Type	**#**	**b x h x w**	**f_t=P_{max} / 2A_n**
	-	(m)	(N/m^2)
Existing SMM Wall	1	1.20 x 1.20 x 0.45	24,074
	2	1.20 x 1.20 x 0.45	18,518
	3	1.20 x 1.20 x 0.45	18,055
Retrofitted SMM Wall	1	1.20 x 1.20 x 0.50	55,555
	2	1.20 x 1.20 x 0.50	56,018
	3	1.20 x 1.20 x 0.50	55,555

Experimental results showed that all specimens had similar failure mechanisms with cracks beginning in the middle of the panels and then spreading through the mud mortar joints (without damaging the stones) towards the corners supported by steel cradles, leading to the eventual collapse of the samples. The retrofitted samples (with reinforced through concrete elements and cement plaster applied to both faces of the panels) exhibited a diagonal crack on both sides of the panel through the cement plaster but did not collapse. Post-test removal of the plaster layer for the retrofitted wall panels revealed that cracking also occurred through the mortar bed joints for these panels, but there were no cracks observed in the stones. Some wall panels exhibited sliding along horizontal mortar joints at a location approximately 2-3 courses from the top of the panel, prior to the formation of a stepped diagonal crack. For all wall panels, sliding along the mortar bed joints was observed following the formation of diagonally extending cracks.

2.4 Discussion

The first conclusion drawn from the experimental results is that the shear strength of SMM walls is heavily dependent on the mortar resistance, as the cracks propagate mainly through the joints, without damaging the stones. Based on the experimental results, it is noted that the stone arrangement also leads to some differences in masonry strength, particularly if joints lined up that led to sliding failure occurring.

By comparing the Force-Displacement curves (Fig. 7) it can be observed that the behaviour of the existing wall panels is strongly nonlinear, even for low load levels. In each specimen, the experimental response shows an approximately linear response before masonry cracking, followed by a nonlinear response up to the maximum strength. After the peak load is reached, a sudden failure response is observed, which is typical of irregular masonry. A comparison between the existing wall panels and the retrofitted wall panels highlights that, in all cases, the through concrete elements and cement plaster increased the strength of the panels.

3 Numerical Modelling

Due to the random nature of SMM wall construction, and the fact that stones and mortar have different elastic and non-linear properties, analysing a finite element model can be very complex. Generally, three different approaches can be followed for numerical modelling and analysis: micro-modelling, simplified mico-modelling and macro-modelling [9]. Micro and simplified mico-modelling require that the individual stones, the mortar joints and their interfaces are all modelled, and thus setting up these 3D models and running the analysis usually takes a very long time. A simplified micro-modelling approach was adopted by [6] using the same experimental information, and thus for this paper it was decided to adopt a macro-modelling approach to compare the results between both analyses. Thus, the stones, mortar joints and interfaces were globally represented by single continuous elements and average parameters were calibrated for these elements based on laboratory experiments. [4]

ANSYS was chosen to carry out this macro-finite element modelling, as it allows for nonlinear behaviour to be simulated through the use of different material models. In this case a combination of Drucker-Prager (DP) plasticity and Willam-Warnke (WW) failure criteria were used to reproduce the constitutive behaviour of the masonry, assuming an elastoplastic law with tension cut-off. Three-dimensional finite element models of the laboratory experiments were created in ANSYS [10] with the aim of replicating their plastic deformation and failure mechanisms. This resulted in a calibrated nonlinear material model which could then be used to simulate the behaviour of other structures built from SMM.

3.1 Previous Research

Both the DP and the WW criteria have been used extensively in previous analyses, to model the nonlinear behaviour of unreinforced masonry buildings. Lourenco et. al. [11] used the DP model to simulate the plastic deformation of masonry cells and showed that it is possible to account for the degradation of the masonry mechanical properties under compression. Adam et. al. [12] adopted the WW failure criteria to model cracking and crushing phenomena, and they were able to produce good agreement between the numerical and experimental results. The two models were combined by Chiostrini et. al. [3] to reproduce the results of several diagonal tests on masonry panels, and they were able to achieve good agreement with the experimental results. Finally, Betti et. al. [13, 14] combined DP and WW criteria to evaluate the seismic vulnerability of a masonry church, confirming that this method can be used to simulate entire buildings.

The combination of the DP plasticity model with the WW failure criteria allows for the introduction of a cut-off to the tensile strength (simulating elastic-brittle behaviour) and an upper limit to the biaxial compressive strength (simulating elastoplastic behaviour). In practice this translates to a material with small tensile strength, plastic behaviour under average compression and crushing under high compressive stresses.

3.1.1 Drucker-Prager Plasticity

The classic Drucker-Prager model is applicable to granular (frictional) material such as soils, rock and concrete and its yield surface can be considered as a smooth version of the Mohr-Coulomb yield surface. Typically the parameters c (cohesion) and ϕ (internal friction angle) are introduced in such a way that the circular cone of DP in the principal stress space corresponds to the outer vertex of the hexagonal Mohr-Coulomb yield surface. The DP model allows for the plasticity of the material to be taken into account and requires only three constants to be defined, as shown in Table 3.

Table 3 – Constants required to define the Drucker-Prager plasticity model.

Constant	**Symbol**	**Units**
Cohesion Value	C	N/mm^2
Angle of Internal Friction	Φ	Degrees
Dilatancy Angle	Δ	Degrees

While the Drucker-Prager model accurately simulates the plastic nature of the material it does not include failure criteria in tension and compression. These failure criteria are taken into account by adding the Willam-Warnke Concrete model to the analysis.

3.1.2 Willam-Warnke Failure Criteria

The Willam-Warnke concrete model allows for cracking in three orthogonal directions, crushing, and plastic deformation to be taken into account with the user defining the material tensile and compressive stresses. Rather than simulating the initiation and propagation of dominant cracks, the smeared crack model is used which is based on the idea that many small cracks form in a material and that these only form one or more dominant cracks at a later stage of the loading process. Since each individual crack is not numerically resolved, the smeared crack model captures the deterioration process through a constitutive relation, thus smearing out the cracks over the continuum. [15]

This model requires four constants to be defined: f_{cWW}, f_{tWW}, βt and βc. f_{cWW} and f_{tWW} represent the ultimate compressive and tension forces (respectively) at which failure will occur while βt and βc account for a shear strength reduction of the stress, producing sliding across the crack face for open (βt) and re-closed cracks (βc) [10]. A value of 0.15 was used for the shear coefficient of cracking which implies that the cracked section has 15% capacity of the original un-cracked section, and a value of 0.75 was used for the compression transfer coefficient in crushing which implies that the crushed section has 75% capacity of the original uncrushed section. [16]

Table 4 – Parameters for the Willam-Warnke concrete model.

Constant	**Symbol**	**Units**
Compressive Strength	f_{cWW}	MPa
Tensile Strength	f_{tWW}	MPa
Shear Transfer (closed crack)	β_c	-
Shear Transfer (open crack)	β_t	-

3.2 Calibration of the Material Model

As noted above, the first step in the creation of a nonlinear material model is to perform a careful calibration exercise to determine accurate mechanical parameters for the masonry assemblage. The material model used in this paper was calibrated based on the experimental results discussed previously, and this section lists the steps involved in this process.

3.2.1 Setup of the Numerical Models

Exact three-dimensional finite element models of the laboratory experiments were created and these were subjected to the same forces and boundary conditions as in the experiments. Based on a sensitivity analysis, the mechanical properties of these models were then calibrated until the plastic deformation and failure mechanisms in the numerical models matched what was measured or observed in the laboratory experiments.

This numerical simulation was carried out using ANSYS code ver. 18.1 [10] and the panels were modelled using eight-node isoparametric plane stress elements (SOLID65). A typical finite element discretisation of the masonry panels and steel apparatus used in the study is shown in Fig. 6. The steel sections were modelled as an elastic material while the masonry was modelled as an isotropic continuum.

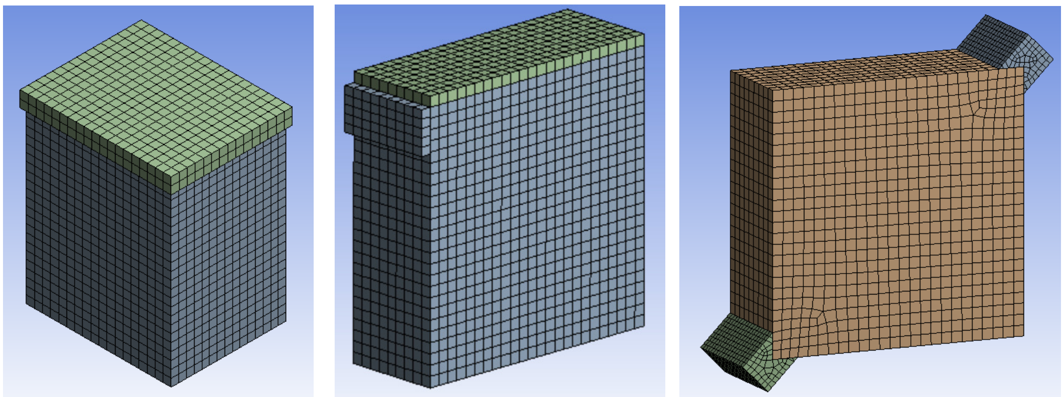

Fig. 6 – A finite element discretisation of the masonry panels used in the uniaxial compression test (left), combined axial and shear tests (middle) and diagonal compression test (right) numerical analyses.

3.2.2 Initial material model parameter values

The material model was initially set up using parameters calculated from the laboratory experiments and from a literature review as shown in Table 5. Thus the modulus of elasticity (E) for both types of samples was set at 60 MPa in the numerical model in line with the findings from Section 4.1.2, and the compressive and tensile strengths of the material were based on the results from the uniaxial tests and diagonal compression tests respectively. The values for Poisson's ratio, internal angle of friction, dilatancy angle and cohesion were all initially set to values based on a literature review. [5]

A sensitivity analysis was then completed to see how varying each of the parameters changed the behaviour of the numerical models under loads. This sensitivity analysis was conducted manually and was very time consuming as it was necessary to determine the value of the numerous material model parameters which correlated with all of the different experimental results. This process revealed that in order to achieve a more accurate result with the numerical models the values for the internal angle of friction, cohesion, dilatancy angle and the ultimate compressive capacity should all be increased, as shown in Table 5.

3.2.3 Comparison of laboratory experiment results and output from the numerical simulations

A sensitivity analysis was then completed to see how varying each of the parameters changed the behaviour of the numerical models. Based on the experimental results, literature review and calibration process, the values summarised in Table 5 were adopted for the various parameters associated with the nonlinear stone masonry in mud mortar material model.

Table 5 – Calibrated values for the parameters associated with the nonlinear SMM material model.

Phase	Parameters	Symbol	units	Initial Values	Calibrated SMM	Calibrated Retrofit
Elastic	Young's Modulus	E	MPa	60	60	60
	Poisson's Ratio	v	-	0.25	0.44	0.44
Plastic	Cohesion	C	MPa	0.1	0.2	0.2
	Internal Friction	Φ	°	35	55	55
	Dilatancy Angle	Δ	°	15	25	25
Failure	Compressive Strength	f_{cWW}	MPa	2.4	4	4
	Tensile Strength	f_{tWW}	MPa	0.02	0.02	0.06
	Shear Transfer (closed)	β_c	-	0.75	0.75	0.75
	Shear Transfer (open)	β_t	-	0.15	0.15	0.15

3.2.4 Numerical Simulation of the Uniaxial Compression Test

Fig. 7a shows the force-displacement curves for the uniaxial compression tests on three different existing SMM wall panels. These curves were used to calibrate the constitutive nonlinear material model in ANSYS, with a close correlation being achieved.

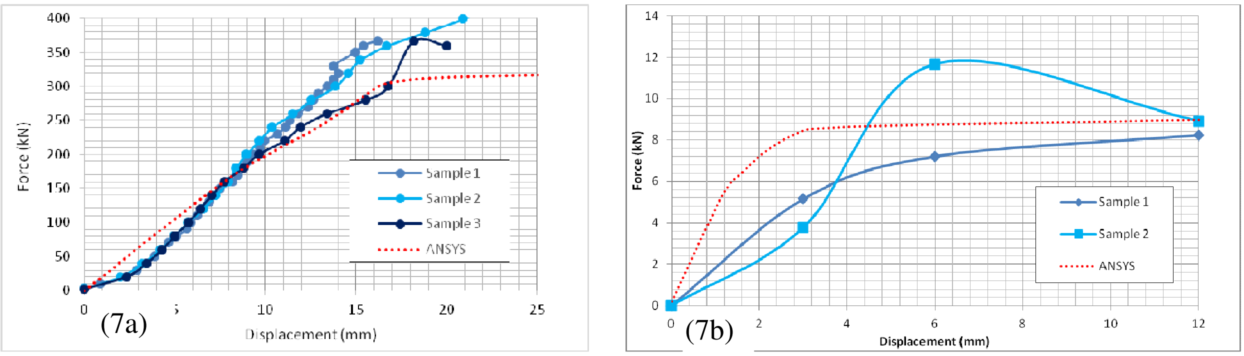

Fig. 7 – Comparison of the force-displacement plots between the experimental results and the numerical simulation output for the uniaxial compression test (a) and the combined axial and shear test (b).

3.2.5 Numerical Simulation of the Combined Axial and Shear Test

Fig. 7b shows the force-displacement graphs for the combined axial and shear tests on two different existing SMM wall panels. For this calibration exercise the first three displacement/force points were used in one direction to generate a force-displacement graph, and the constitutive nonlinear material model in ANSYS was calibrated, until a close correlation was achieved. Fig. 8 shows how the damage pattern in the FEA model closely matches the crack patterns observed in the laboratory panels at failure.

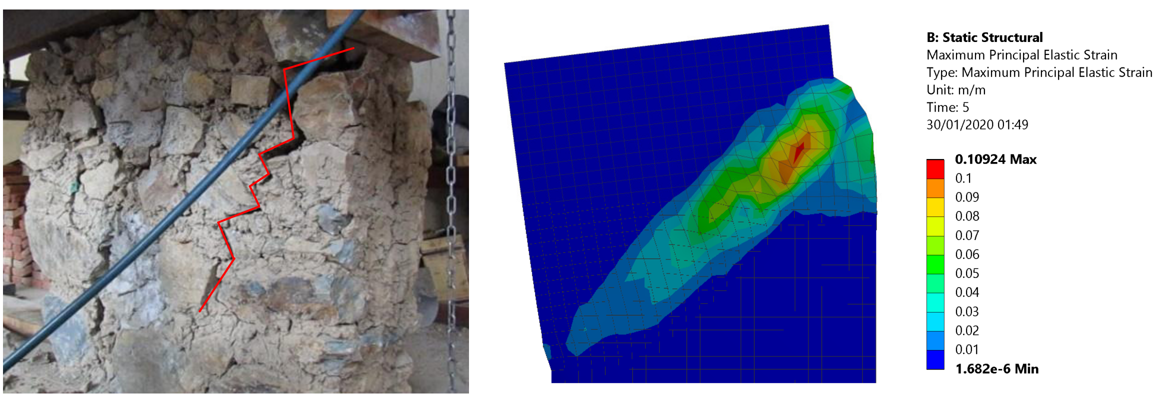

Fig. 8 – Similar failure/crack patterns between the experimental observations and the FEA model output.

3.2.6 Numerical Simulation of the Diagonal Compression Tests

The diagonal compression test was very important for the creation of an accurate material model as it allowed for the tensile capacity of the masonry to be calculated. According to the results obtained with the finite element method, which are shown in Fig. 9, a reasonable matching between numerical and experimental values for the nonlinear behaviour of the material was obtained. The numerical model shows a change from elastic to plastic behaviour at approximately the same force as the experiments although the numerical model does not show as much deflection during the elastic phase. The change in slope could be due to the experimental apparatus with elongation of the steel cables and bending of the steel beams both possible sources of additional displacement. In addition, the nature of the physical samples could also have an effect, with small gaps between the rocks or sliding along mortar joints leading to additional displacement that the numerical model does not account for. This appears to be the case for SMM Sample 2 at a force of approximately 13kN and for the retrofitted Sample 1 for a force of approximately 5kN.

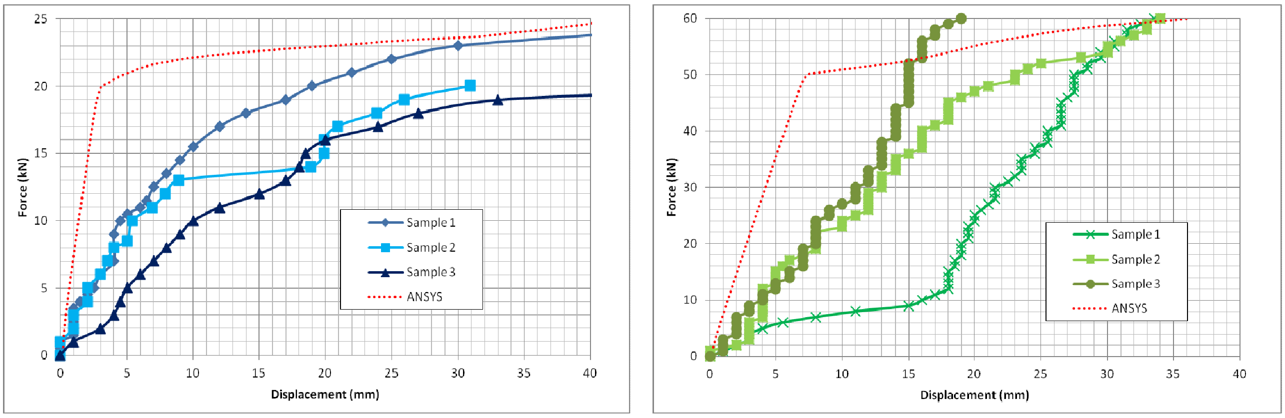

Fig. 9 – Experimental and numerical results for existing SMM panels (left) and retrofitted panels (right).

Additionally, the failure mode of the numerical models agrees reasonably well with the experimental results for both sample types. As shown in Fig 10 the numerical results showed similar crack patterns developing during the experimental behaviour of the wall, as the compression load approaches 20 kN. The cracks observed in the experimental sample panel, and the cracks predicted by the ANSYS model, were both approximately 10mm wide showing a good correlation between the laboratory experiment results and the simulated numerical model output.

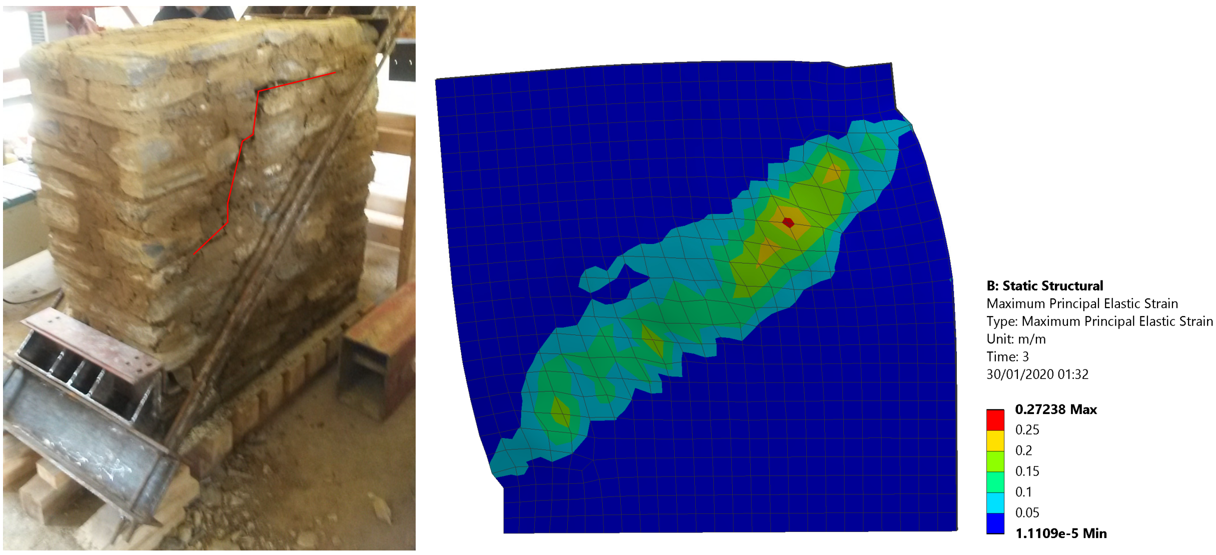

Fig. 10 – Experimental panel crack pattern (left) and numerically predicted crack pattern (right).

4 Conclusions and Future Work

An experimental research campaign on the behaviour of both existing and retrofitted SMM panels tested in uniaxial compression, combined axial and shear and diagonal compression has been presented. Based on the results obtained from the experimental programme, supported by the calibration of a corresponding constitutive nonlinear material model for detailed numerical analysis, the conclusions below can be made:

- The uniaxial compression tests allowed for accurate values for the ultimate compression capacity and modulus of elasticity to be estimated. The stress-strain behaviour of the samples was also recorded and this, along with observations, provided valuable insight into ultimate compression failure mechanisms.
- The combined axial and shear tests and diagonal compression tests allowed for the shear strength and tensile strength of both types of samples to be determined and the stress-strain curves, along with observations, provided valuable insight into the sudden brittle failure mechanisms associated with tensile failure.
- Numerical analysis was then performed by finite element models, to simulate the nonlinear behaviour of the masonry samples and a constitutive nonlinear material model for SMM walls and retrofitted walls was calibrated. In this paper, the force-displacement diagrams and failure modes were the main aspects under analysis and good matching between the numerical models and the experimental results was obtained in both cases. In addition, the crack patterns obtained by numerical analyses were similar to the crack patterns obtained by experimental results at the same loads.
- The laboratory experiments and numerical analysis confirmed that the retrofit approach adopted by Build Change (concrete plaster and through concrete elements) increases the tensile and shear capacity of SMM walls by approximately three times.
- The constitutive nonlinear material models developed in this paper will be used in a subsequent paper to analyse FEA models of traditional SMM buildings in Nepal to determine their seismic capacity. These FEA models will then be strengthened using Build Change's retrofit design and analysed to determine what effect this retrofit has on their seismic capacity.

5. Acknowledgements

The authors would like to express appreciation to the following people for their contributions to the preparation of this paper. Carlos Andres Arce for his assistance with learning the software ANSYS and how to implement nonlinear material models. Saugat Shrestha and Binaya Paudel for their assistance with setting up the laboratory experiments, conducting the tests and recording the results. Aning Kuswinarni for her assistance with creating the figures used and Tim Hart and Michael Meadows for carrying out final edits of the paper.

6. References

[1] ASTM E 519-81 (1981). Standard Test Method for Diagonal Tension (Shear) in Masonry Assemblages, *American Society for Testing Materials*, USA.

[2] Brignola, A. Podestà, S. Lagomarsino, S. (2006): Experimental Results of Shear Strength and Stiffness of Existing Masonry Walls. *In Structural Analysis of Historical Constructions*, New Delhi, India.

[3] Chiostrini, S. Galano, L. Vignoli, A. (1998): In-situ tests and numerical simulations on structural behaviour of ancient masonry. *In Proceedings of Monument-98, Workshop on Seismic Performance of Monuments 12-14 November 1998*, Lisbon, Portugal.

[4] Betti, M. Galano, L. Vignoli, A. (2015): Finite element modelling for seismic assessment of historic masonry buildings, *Earthquakes and Their Impact on Society, Springer International Publishing*, Switzerland.

[5] Dizhur, D. Ingham, J. (2013): Diagonal tension strength of vintage unreinforced clay brick masonry wall panels, *Construction and Building Materials – June*, Department of Civil and Environmental Engineering, The University of Auckland, New Zealand.

[6] Adhikari, R. K. D'Ayala, D. (2019): 2015 Nepal Earthquake: Seismic Performance and Post-Earthquake Reconstruction of Stone Masonry Buildings, *EEFIT Project Report*, Department of Civil, Environmental and Geometic Engineering, University College London, England.

[7] ASTM E C1314-18 (2018). Standard Test Method for Compressive Strength of Masonry Prisms, *American Society for Testing Materials*, USA.

[8] Chiostrini, S. Galano, L. Vignoli, A. (2000): On the determination of strength of ancient masonry walls via experimental tests, *12th World Conference on Earthquake Engineering*, Auckland, New Zealand.

[9] Lourenco, P. B. (1998): Experimental and numerical issues in the modeling of the mechanical behavior of masonry, *Structural Analysis of Historical Constructions II*, CIMNE, Barcelona, Spain.

[10] ANSYS Inc. (1998): ANSYS manual, Southpoint, USA.

[11] Lourenco, P. B. et. al. (2007): Analysis of masonry structures: review of the recent trends in homogenization techniques, *Canadian Journal of Civil Engineering 34*, 1443-1457, Canada.

[12] Adam, J. et. al. (2009): Axially loaded RC columns strengthened by steel caging. Finite element modeling. Construction and Building Materials, 23(6), 2265-2276

[13] Betti, M. Vignoli, A. (2008). Modelling and analysis of a Romanesque church under earthquake loading: *Assessment of seismic resistance*. Engineering Structures, 30(2), 352–367.

[14] Betti, M. Galano, L. Vignoli, A. (2016). Finite Element Modelling for Seismic Assessment of Historic Masonry Buildings, *Earthquakes and Their Impact on Society*, Springer International Publishing, Switzerland.

[15] De Borst, R. et. al. (2004). Discrete vs smeared crack models for concrete fracture: bridging the gap, Numerical and Analytical Methods in Geomechanics, John Wiley & Songs, Ltd, USA.

[16] Betti, M. Galano, L. Vignoli, A. (2015). Time-History Seismic Analysis of Masonry Buildings: A Comparison between Two Non-Linear Modelling Approaches, Buildings, 5, 597-621.

